JOURNAL OF THE ROYAL SOCIETY Interface

rsif.royalsocietypublishing.org

Research

Cite this article: Hirata H, Chiam K-H, Lim CT, Sokabe M. 2014 Actin flow and talin dynamics govern rigidity sensing in actin–integrin linkage through talin extension. *J. R. Soc. Interface* **11**: 20140734.
http://dx.doi.org/10.1098/rsif.2014.0734

Received: 6 July 2014
Accepted: 30 July 2014

Subject Areas:
biophysics, biomechanics

Keywords:
focal adhesion, mechanosensor, mechanotransduction, substrate stiffness, talin, vinculin

Authors for correspondence:
Keng-Hwee Chiam
e-mail: chiamkh@bii.a-star.edu.sg
Masahiro Sokabe
e-mail: msokabe@med.nagoya-u.ac.jp

Royal Society Publishing

Actin flow and talin dynamics govern rigidity sensing in actin–integrin linkage through talin extension

Hiroaki Hirata[1], Keng-Hwee Chiam[1,2], Chwee Teck Lim[1,3,4] and Masahiro Sokabe[1,5]

[1]Mechanobiology Institute, National University of Singapore, Singapore 117411, Singapore
[2]A*STAR Bioinformatics Institute, Singapore 138671, Singapore
[3]Department of Biomedical Engineering, and [4]Department of Mechanical Engineering, National University of Singapore, Singapore 117576, Singapore
[5]Mechanobiology Laboratory, Nagoya University Graduate School of Medicine, Nagoya 466-8550, Japan

At cell–substrate adhesion sites, the linkage between actin filaments and integrin is regulated by mechanical stiffness of the substrate. Of potential molecular regulators, the linker proteins talin and vinculin are of particular interest because mechanical extension of talin induces vinculin binding with talin, which reinforces the actin–integrin linkage. For understanding the molecular and biophysical mechanism of rigidity sensing at cell–substrate adhesion sites, we constructed a simple physical model to examine a role of talin extension in the stiffness-dependent regulation of actin–integrin linkage. We show that talin molecules linking between retrograding actin filaments and substrate-bound integrin are extended in a manner dependent on substrate stiffness. The model predicts that, in adhesion complexes containing ≈30 talin links, talin is extended enough for vinculin binding when the substrate is stiffer than 1 kPa. The lifetime of talin links needs to be 2–5 s to achieve an appropriate response of talin extension against substrate stiffness. Furthermore, changes in actin velocity drastically shift the range of substrate stiffness that induces talin–vinculin binding. Our results suggest that talin extension is a key step in sensing and responding to substrate stiffness at cell adhesion sites.

1. Introduction

The importance of stiffness or rigidity of extracellular substrates has been demonstrated in a wide variety of cellular functions, including adhesion, migration, morphogenesis, proliferation and differentiation [1]. A soft substrate with elastic modulus (E) of 0.1–1 kPa leads to neurogenic differentiation of mescenchymal stem cells, but stiffer substrates with E of 8–12 kPa and 25–40 kPa lead to myogenic and osteogenic differentiation, respectively [2]. When plated on the substrate with a gradient of stiffness, fibroblasts and smooth muscle cells migrate towards stiffer regions [3–5]. These cells spread and develop actin stress fibres when they are on substrates with $E \geq 5$ kPa, but do not when $E \approx 1$ kPa or less [6–8].

How do cells detect substrate stiffness? Cells adhere to substrates mainly through the adhesion complexes mediated by integrins, receptors for extracellular matrices [9]. These complexes serve as a mechanical connection between the actin cytoskeleton network and the extracellular substrate, and, therefore, their involvement in rigidity sensing has been appreciated [10–12]. Actomyosin-generated contractile forces are transmitted through the adhesion complexes to the substrate, causing deformation of compliant substrates [13–17]. If cells can measure the force-induced deformation of the substrate, they will be able to sense stiffness of the substrate.

Integrins are clustered at the adhesion complexes. Actomyosin forces cause a retrograde movement of actin filaments with respect to the integrin clusters. The

© 2014 The Author(s) Published by the Royal Society. All rights reserved.

moving actin filaments are dynamically linked to integrin clusters through association/dissociation of linker proteins [18,19], which has been modelled as a molecular clutch [20,21]. When the substrate is stiff enough ($E \geq 5$ kPa), the actin–integrin linkage is strengthened, and the adhesion complexes are stabilized [6,8,22]. Assuming that dissociation rates of molecular links are increased by mechanical forces loaded to the links, the clutch model has successfully related the elastic deformation of substrates with breakages of the linkage [21,23]. However, these modelling studies have not revealed molecular identities responsible for detecting the substrate deformation in terms of stiffness sensing.

The linker protein talin has both β-integrin- and actin-binding sites [24] and is responsible for the formation of the initial link between actin filaments and integrin at cell adhesion sites [25–27]. However, the talin-mediated link is broken by a small force of approximately 2 pN generated by the retrograding actin filaments [26]. Another linker protein vinculin binds to actin and talin and reinforces the actin–integrin linkage [28–30]. When binding of vinculin with talin is inhibited, actin filaments slip over integrin clusters [31]. Importantly, vinculin binding with talin depends on mechanical extension of talin [32–34]. Talin has multiple vinculin-binding sites, and they are buried in the bundles of amphipathic helices of a talin molecule [35,36]. However, these sites are exposed when the talin molecule is extended [32–34]. If talin extension is influenced by deformation of the substrate, talin and vinculin potentially regulate actin–integrin linkage in a manner dependent on substrate stiffness.

In this study, we examine a possible role of talin extension in stiffness-dependent reinforcement of actin–integrin linkage using a simple mechanical model. We show that talin molecules linking between moving actin filaments and integrin bound to the elastic substrate are extended in a substrate stiffness-dependent manner. We further reveal that the lifetime of the talin link and the velocity of actin movement are critical for the stiffness-dependent regulation of talin extension and talin–vinculin binding.

2. Model

2.1. Single molecules model

As the simplest case, we consider the system in which a single talin molecule with a spring constant k_T links an actin filament moving at a velocity v to an integrin molecule bound to the substrate. The single talin link has the intrinsic lifetime of $\tau \approx 3$ s [26]. When the talin link is extended by the moving actin filaments ($v \approx 70$ nm s^{-1}) [22,26,31] during the lifetime of the link, the force loaded to the link reaches $f \approx 2$ pN [26]. Therefore, the apparent spring constant of a talin molecule is estimated as $k_T = f/v\tau \approx 0.01$ pN nm^{-1}. When the substrate is elastic and has a spring constant k (figure 1*a*), the change in the molecular length of talin (Δl) is expressed as a function of time (t) after the formation of the link, as

$$\Delta l(t) = \frac{vt}{1 + k_T/k}, \tag{2.1}$$

where $0 \leq t \leq \tau$ (≈3 s). When Δl becomes longer than the critical length (Δl_c), the vinculin-binding site(s) in talin is exposed, and the actin–integrin linkage is reinforced by talin–vinculin binding.

2.2. Cluster model

Integrin molecules are initially clustered as nascent adhesions in a manner independent of actomyosin forces [37,38]. While most of them are disassembled rapidly, the ones which are exposed to actomyosin forces are developed into focal complexes. Focal complexes are major sites for traction force exertion to the substrate in protruding lamellae [39]. Thus, it is plausible that the substrate stiffness-dependent reinforcement of the actin–integrin linkage occurs in the phase of the focal complex formation. We therefore expand the 'single molecules model' to describe extension of talin links at focal complexes, as shown in figure 1*b*.

For simplicity, we first assume that the n talin molecules pull on the integrin cluster in a direction perpendicular to the plane of the substrate. Mechanical stress developed in the substrate at a circular focal complex (diameter a) is

$$P = \frac{nf}{S}, \tag{2.2}$$

where S ($=\pi a^2/4$) is the area of the focal complex. Here, P acts only in the z-direction perpendicular to the plane of the substrate. The displacement at every point in the substrate can then be computed as the solution to the Boussinesq problem [40], except that instead of a point stress, the stress is applied over circular area S. For example, the displacement Δd_i of points (x, y, 0) on the surface of the substrate (i.e. $z = 0$) in the ith direction (where $i = x, y, z$) due to the stress in the z-direction is

$$\Delta d_i(x, y, 0) = \int_0^{2\pi} r\mathrm{d}\theta \int_0^a \mathrm{d}r g_{iz}(r) P, \tag{2.3}$$

where g_{xz}, g_{yz} and g_{zz} are the coefficients of a Green's tensor that give the displacement in the ith direction of a point (x, y, z) in the substrate induced by a point force in the z-direction at the origin. The derivation of the g's is available elsewhere [15,40].

An example of the displacement field for a cross section of the substrate is shown in figure 1*b*, where we plot the magnitude of the displacement,

$$\Delta d(x, y = 0, z) = (\Delta d_x^2 + \Delta d_y^2 + \Delta d_z^2)^{1/2}. \tag{2.4}$$

We can see that the largest displacement occurs underneath the circular disc S. In fact, owing to the azimuthal symmetry of the problem, the maximum magnitude of the displacement Δd_{max} will occur at the centre of the circular disc and only the z component of the displacement will be non-zero,

$$\Delta d_{max} = \Delta d_z(0, 0, 0) = \int_0^{2\pi} r\mathrm{d}\theta \int_0^a \mathrm{d}r \frac{(1-\mu^2)P}{\pi E r} = \frac{8(1-\mu^2)nf}{\pi E a}. \tag{2.5}$$

Here, E and μ are the Young's modulus and Poisson's ratio of the substrate, respectively. For commonly used material like polydimethyl siloxane, $\mu \approx 0.5$, resulting in

$$\Delta d_{max} = \frac{6nf}{\pi E a}. \tag{2.6}$$

We now revisit the validity of one of our assumptions that the stress P acts only in the z-direction. It can be argued that, owing to the tangential actin flow, the stress P exerted on the substrate may be tangential to the substrate instead of being perpendicular to it, as we have considered above. To study this scenario, we now let P act in the x-direction such that

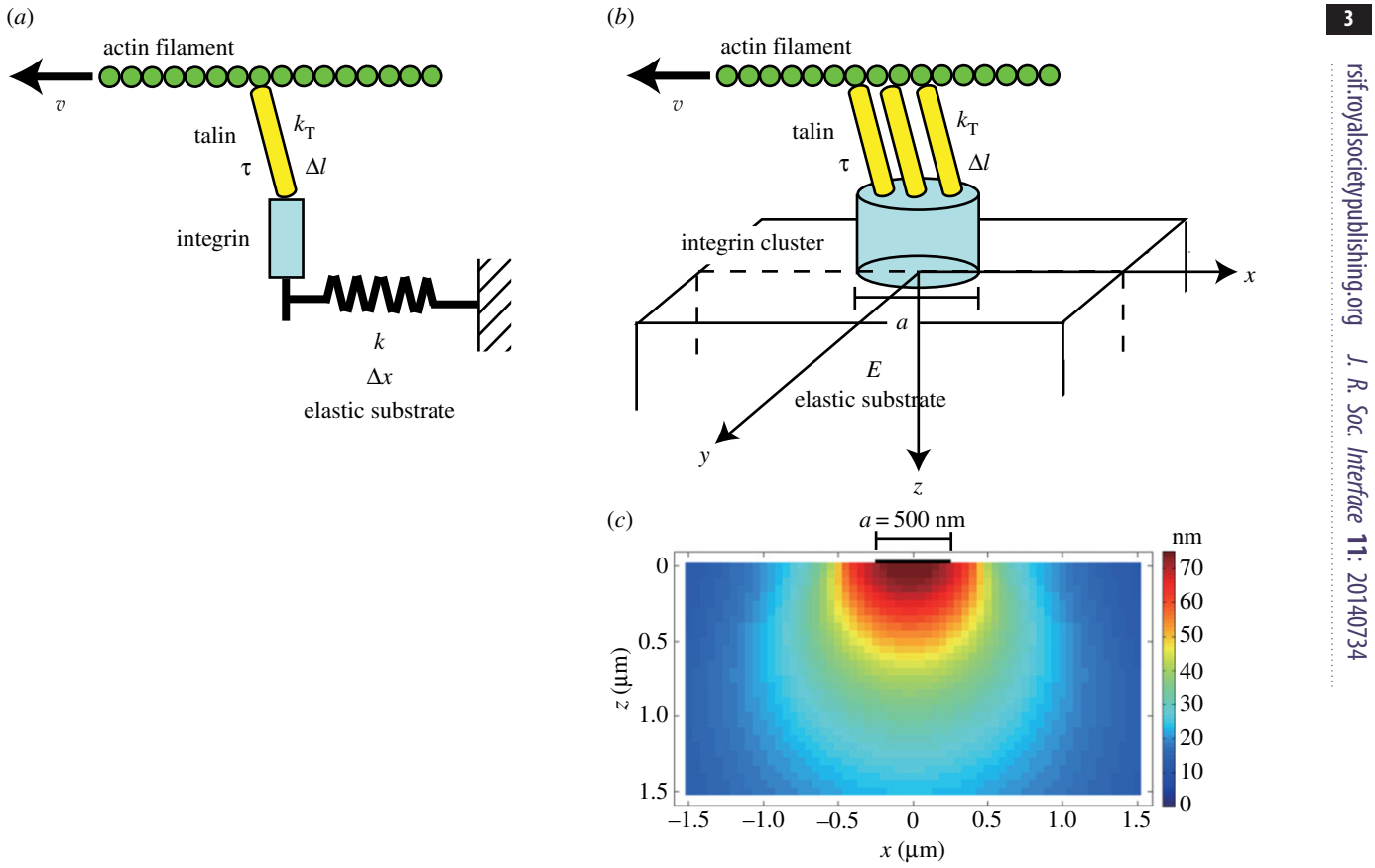

Figure 1. Schematic of the models. (*a*) The single molecules model. A single talin molecule links between an actin filament moving with the velocity v and integrin bound to the elastic substrate with the spring constant k. The talin link, which has the lifetime τ, transmits a force f to the substrate and is extended by Δl between the moving actin filament and the substrate deformed by Δx. (*b*) The cluster model. Multiple talin molecules link between actin filaments moving with the velocity v and an integrin cluster with a diameter a. The integrin cluster is bound to the elastic substrate whose elastic modulus is E. Each talin link has the lifetime τ, transmits a force f to the substrate and is extended by Δl between moving actin filaments and the deformed substrate. (*c*) An example of the displacement field for the x–z cross section (the plane denoted by dotted lines in the (*b*)) of the substrate. The parameters used are $a = 500$ nm, $f = 2$ pN, $n = 10$ and $E = 1$ kPa. The black bar indicates the position of the integrin cluster. (Online version in colour.)

there is no force acting in the y- and z-directions. A similar analysis as above yields $\Delta d_{\max} = \Delta d_x(0, 0, 0)$ instead of $\Delta d_z(0, 0, 0)$. Because $g_{zz} = g_{xx}$ at the centre of the disc (0, 0, 0), we obtain the same result as before,

$$\Delta d_{\max} = \Delta d_x(0, 0, 0) = \frac{8(1-\mu^2)nf}{\pi Ea}. \tag{2.7}$$

Thus, the maximum displacement $\Delta d_{\max}$ is the same for when P is either perpendicular or tangential to the substrate. Therefore, our results derived here will also be valid for the scenario when the stress P caused by the pulling force through talin is fully tangential.

Talin molecules at a focal complex will be extended between actin filaments moving at the velocity v and the integrin cluster bound to the elastic substrate. From equation (2.6), extension of the talin link is expressed as a function of time (t) after the formation of the link, as

$$\Delta l(t) = vt - \Delta d_{\max}(t) = vt - \frac{6nk_T\Delta l(t)}{\pi Ea}. \tag{2.8}$$

That is,

$$\Delta l(t) = \frac{vt}{(1 + 6nk_T/\pi Ea)}, \tag{2.9}$$

where $0 \le t \le \tau$ (≈3 s). Similarly to the case of the 'single molecules model', the link is reinforced by the vinculin binding with talin when $\Delta l \ge \Delta l_c$.

3. Results and discussion

With the cluster model expressed by equation (2.9), we first examined the relationship between substrate stiffness and extension of talin links at focal complexes. Considering the velocity of actin filaments at focal complexes ($v \approx 70$ nm s^{-1}) [22,26,31] and the size of focal complexes ($a \approx 500$ nm) [41], extension of talin links at the end of their lifetime ($t = 3$ s) was calculated as a function of substrate stiffness, as shown in figure 2*a*. In each case with the different n value, the length of talin extension is increased to the plateau value ($v\tau \approx 210$ nm) with increasing stiffness of the substrate. In living cells, the actomyosin-dependent binding of vinculin to talin at adhesion sites associates with extension of talin by 100–350 nm [42], suggesting that the critical length of talin extension (Δl_c) which induces vinculin binding and concomitant reinforcement of the actin–integrin linkage is ≈100 nm. Substrates stiffer than 1 kPa are required for reinforcing the linkage and thereby stabilizing adhesions and ensuring cell spreading [6–8,22]. On the other hand, according to the result shown in figure 2*a*, when the number of talin links

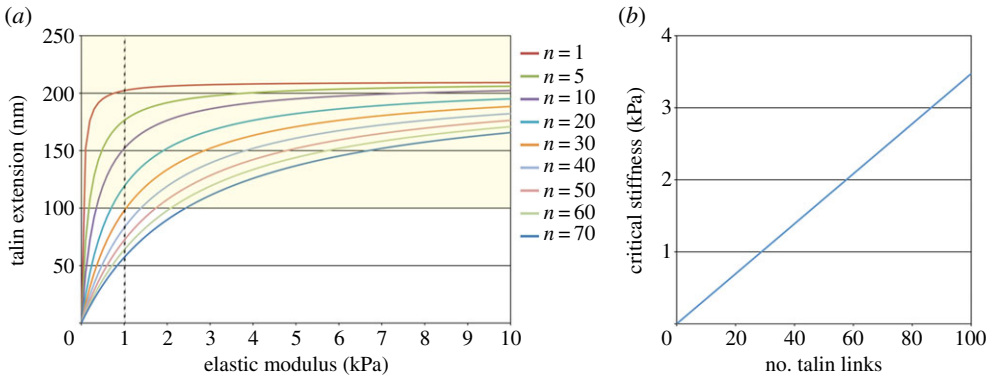

Figure 2. Talin links are extended in a substrate stiffness-dependent manner. (*a*) The relationship between extension of talin links at the end of their lifetime ($t = 3$ s) and substrate stiffness. Traces for focal complexes (500 nm in diameter) with the different number of talin links are shown. The order of traces is the same as that of legends. In each trace, the length of talin extension is increased to the plateau value ($v\tau \approx 210$ nm) with increasing stiffness of the substrate. When talin links are extended by more than or equal to 100 nm (yellow zone), vinculin binds to talin. (*b*) The critical stiffness of the substrate which yields 100 nm extension of talin links varies with the number of talin links in a focal complex. (Online version in colour.)

in a focal complex is too small ($n < 20$), talin molecules are extended by more than 100 nm, and therefore the actin–integrin linkage will be reinforced by vinculin, even on the substrate softer than 1 kPa. From equation (2.9), the substrate stiffness yielding the critical talin extension ($\Delta l_c = 100$ nm) varies linearly with the number of talin links (figure 2*b*), as

$$E = \frac{n \times (6k_T/\pi a)}{(v\tau/\Delta l_c - 1)}. \tag{3.1}$$

To endow the set of critical values of talin extension and substrate stiffness ($\Delta l \approx 100$ nm, $E \approx 1$ kPa) which were obtained in living cells, the number of talin links in a focal complex was estimated in our model as approximately 30 (figure 2*b*). Importantly, the estimated number of talin links is comparable to the number calculated from the reported experimental data; the magnitude of force exerted to the substrate through a focal complex is 50–80 pN [22,43], which corresponds to 25–40 talin links if each link transmits a force of 2 pN, as reported elsewhere [26].

We next investigated the influence of talin dynamics on the stiffness-dependent talin extension. The result for a focal complex containing 30 talin links is shown in figure 3. When the lifetime of the talin link is less than or equal to 1 s, talin molecules are not extended by 100 nm during their lifetime, i.e. they do not get to bind with vinculin, even on the substrates stiffer than 10 kPa. On the other hand, when the lifetime is more than or equal to 6 s, talin molecules are extended beyond the physiological range (100–350 nm) [42] on stiff substrates (figure 3, grey zone). Thus, only a narrow window of the lifetime of talin links ($2\text{ s} \leq \tau \leq 5$ s) renders optimal responses of talin extension and reinforcement of actin–integrin linkage against substrate stiffness, indicating a critical role of talin dynamics in stiffness sensing at adhesion sites.

Finally, the effect of actin movement on sensitivity of the actin–integrin linkage to substrate stiffness was examined. Assuming a focal complex containing 30 talin links, the critical stiffness of substrates which endows 100 nm extension of talin molecules varies with the velocity of actin movement, as shown in figure 4. When the actin velocity drops to half (35 nm s^{-1}) of the normal value (70 nm s^{-1}) [22,26,31], a substrate with 23 kPa stiffness is required for 100 nm extension of talin. On the other hand, when the actin velocity becomes twofold higher (140 nm s^{-1}), talin molecules are extended

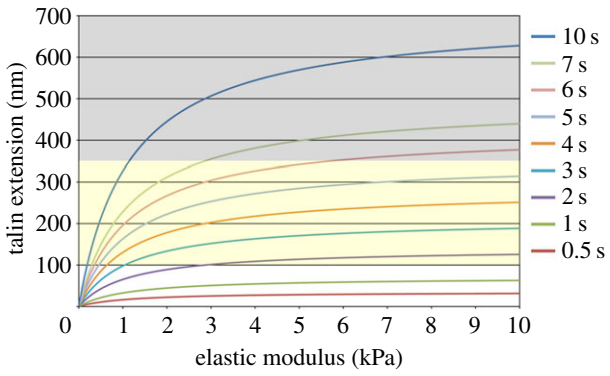

Figure 3. Influence of the lifetime of talin links on the stiffness-dependent talin extension. Each trace represents extension of talin links at the end of their lifetime. The order of traces is the same as that of legends. The results for the focal complex (500 nm in diameter) containing 30 talin links are shown. In each trace, the length of talin extension is increased to the plateau value ($=v\tau$) with increasing stiffness of the substrate. The yellow zone ($100\text{ nm} \leq \Delta l \leq 350$ nm) represents the range where talin links are extended to allow vinculin binding, and the grey zone ($\Delta l > 350$ nm) represents the range where they are extended beyond the level observed in living cells. (Online version in colour.)

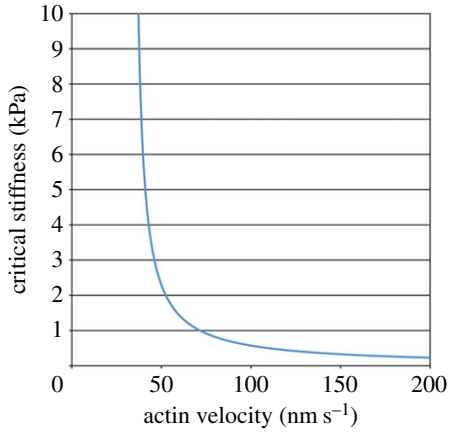

Figure 4. The critical stiffness of the substrate which yields 100 nm extension of talin links varies with the velocity of actin filament movement. The result for the focal complex (500 nm in diameter) containing 30 talin links is shown. (Online version in colour.)

by 100 nm even on a very soft substrate ($E \approx 0.4$ kPa). This result reveals that changes in actin velocity shift critical stiffness of substrates that induce reinforcement of the actin–integrin linkage.

In this study, we showed that talin molecules linking between actin filaments and integrin can be extended in a manner dependent on substrate stiffness. Here, talin works as a dynamic molecular ruler measuring the difference between the travel distance of actin filaments and deformation of the elastic substrate. Our simple model is able to reproduce quantitatively the cellular response against substrate stiffness; talin molecules in the focal complex containing ≈30 talin links are extended enough ($\Delta l \geq 100$ nm) for allowing vinculin binding and concomitant reinforcement of actin–integrin linkage when cells are on substrates stiffer than 1 kPa. Furthermore, we have revealed that the lifetime of the talin link is critical to obtain the optimal dependency of talin extension on substrate stiffness. Real talin links have a typical lifetime of 3 s [26], and our results predict that the acceptable variation in the lifetime is less than 2 s. Thus, our practical approach quantitatively shows that talin has ideal properties to enable the stiffness-dependent regulation of actin–integrin linkage.

Our results have demonstrated that the lifetime of the talin link and the velocity of actin flow are critical parameters in determining critical stiffness of substrates that induce talin–vinculin binding. It is, therefore, predicted that by changing these parameters experimentally, we may be able to modulate responses of talin–vinculin binding against substrate stiffness. For example, if the lifetime of the talin link is prolonged by introducing the mutant form of talin which has high affinity to actin filaments [44], talin would be extended enough for vinculin binding, thereby reinforcing the actin–integrin linkage and enabling cell spreading, even on substrates softer than 1 kPa. Increasing the velocity of the actin flow by upregulating actomyosin activity [45] may also lead to a similar result. As a difference in cell spread area has great influence on gene expression and cell differentiation [46,47], modulation of cell spreading by changing the parameters which affect talin extension would tune the cell differentiation pattern directed by substrate stiffness [2].

We have dealt only with talin extension events driven by a small force of less than or equal to 2 pN, because each talin link in living cells can withstand a force up to 2 pN without reinforcement of the link [26]. *In vitro* analyses of talin–vinculin binding have demonstrated that this magnitude of force can induce vinculin binding to talin [34]. On the other hand, without reinforcement, simple talin links cannot sustain forces required for cell spreading due to weak talin–actin bonds [26,31]. Once vinculin binds to talin, the talin–actin bond is reinforced by actin–vinculin–talin binding [30,31]. The vinculin-reinforced talin links should have a longer lifetime and withstand larger forces compared with simple talin links. Therefore, vinculin binding with talin will enable talin molecules to be extended to a greater extent, leading to exposure of more vinculin-binding sites in talin and more vinculin bindings with talin. Such positive feedback would ensure engagement of actin–integrin linkage and, thereby, cell spreading.

While this study focuses on the reinforcement event of actin–integrin linkage at nascent adhesion complexes, adhesion structures in living cells exhibit multiple responses with different time courses against substrate stiffness. Once actin–integrin linkage is engaged through vinculin-mediated reinforcement, the velocity of retrograde movement of actin filaments is reduced, and the force transmission from actin cytoskeleton to the substrate is increased [30,31]. Subsequently, adhesion complexes grow in size when the substrate is rigid [6,7,17,48]. Physical models have been proposed to account for the stiffness-dependent regulations of force transmission and adhesion growth [21,23,49–51]. However, in these models, specific physical properties of each adhesion and/or adaptor protein are not apparently involved. Further studies, both experimental and theoretical ones, are needed to obtain the mechanotransduction models that are more realistic in terms of the molecular composition and architecture of adhesions and integrate different stages of responses against substrate stiffness.

Funding statement. This work was supported by the Seed Fund from the Mechanobiology Institute at the National University of Singapore and Grant-in-Aid from the Ministry of Education, Culture, Sports, Science, and Technology, Japan under grant nos. 15086207, 16GS0308, 21247021, 24247028 (to M.S.).

References

1. Discher DE, Janmey P, Wang YL. 2005 Tissue cells feel and respond to the stiffness of their substrate. *Science* **310**, 1139–1143. (doi:10.1126/science.1116995)
2. Engler AJ, Sen S, Sweeney HL, Discher D. 2006 Matrix elasticity directs stem cell lineage specification. *Cell* **126**, 677–689. (doi:10.1016/j.cell.2006.06.044)
3. Lo CM, Wang HB, Dembo M, Wang YL. 2000 Cell movement is guided by the rigidity of the substrate. *Biophys. J.* **79**, 144–152. (doi:10.1016/S0006-3495(00)76279-5)
4. Zaari N, Rajagopalan P, Kim SK, Engler AJ, Wong JY. 2004 Photopolymerization in microfluidic gradient generators: microscale control of substrate compliance to manipulate cell response. *Adv. Mater.* **16**, 2133–2137. (doi:10.1002/adma.200400883)
5. Isenberg BC, DiMilla PA, Walker M, Kim S, Wong JY. 2009 Vascular smooth muscle cell durotaxis depends on substrate stiffness gradient strength. *Biophys. J.* **97**, 1313–1322. (doi:10.1016/j.bpj.2009.06.021)
6. Pelham Jr RJ, Wang YL. 2005 Cell locomotion and focal adhesions are regulated by substrate flexibility. *Proc. Natl Acad. Sci. USA* **94**, 13 661–13 665. (doi:10.1073/pnas.94.25.13661)
7. Engler A, Bacakova L, Newman C, Hategan A, Griffin M, Discher D. 2004 Substrate compliance versus ligand density in cell on gel responses. *Biophys. J.* **86**, 617–628. (doi:10.1016/S0006-3495(04)74140-5)
8. Yeung T *et al*. 2005 Effects of substrate stiffness on cell morphology, cytoskeletal structure, and adhesion. *Cell Motil. Cytoskeleton* **60**, 24–34. (doi:10.1002/cm.20041)
9. Geiger B, Spatz JP, Bershadsky AD. 2009 Environmental sensing through focal adhesions. *Nat. Rev. Mol. Cell Biol.* **10**, 21–33. (doi:10.1038/nrm2593)
10. Moore SW, Roca-Cusachs P, Sheetz MP. 2010 Stretchy proteins on stretchy substrates: the important elements of integrin-mediated rigidity sensing. *Dev. Cell* **19**, 194–206. (doi:10.1016/j.devcel.2010.07.018)
11. Kobayashi T, Sokabe M. 2010 Sensing substrate rigidity by mechanosensitive ion channels with stress fibers and focal adhesions. *Curr. Opin. Cell Biol.* **22**, 669–676. (doi:10.1016/j.ceb.2010.08.023)
12. Plotnikov SV, Pasapera AM, Sabass B, Waterman CM. 2012 Force fluctuations within focal adhesions mediate ECM-rigidity sensing to guide directed cell migration. *Cell* **151**, 1513–1527. (doi:10.1016/j.cell.2012.11.034)
13. Harris AK, Wild P, Stopak D. 1980 Silicone rubber substrata: a new wrinkle in the study of cell locomotion. *Science* **208**, 177–179. (doi:10.1126/science.6987736)

14. Chrzanowska-Wodnicka M, Burridge K. 1996 Rho-stimulated contractility drives the formation of stress fibers and focal adhesions. *J. Cell Biol.* **133**, 1403–1415. (doi:10.1083/jcb.133.6.1403)
15. Dembo M, Wang YL. 1999 Stresses at the cell-to-substrate interface during locomotion of fibroblasts. *Biophys. J.* **76**, 2307–2316. (doi:10.1016/S0006-3495(99)77386-8)
16. Tan JL, Tien J, Pirone DM, Gray DS, Bhadriraju K, Chen CS. 2003 Cells lying on a bed of microneedles: an approach to isolate mechanical force. *Proc. Natl Acad. Sci. USA* **100**, 1484–1489. (doi:10.1073/pnas.0235407100)
17. Trichet L, Digabel JL, Hawkins RJ, Vedula SRK, Gupta M, Ribrault C, Hersen P, Voituriez R, Ladoux B. 2012 Evidence of a large-scale mechanosensing mechanism for cellular adaptation to substrate stiffness. *Proc. Natl Acad. Sci. USA* **109**, 6933–6938. (doi:10.1073/pnas.1117810109)
18. Brown CM, Hebert B, Kolin DL, Zareno J, Whitmore L, Horwitz AR, Wiseman PW. 2006 Probing the integrin-actin linkage using high-resolution protein velocity mapping. *J. Cell Sci.* **119**, 5204–5214. (doi:10.1242/jcs.03321)
19. Hu K, Applegate KT, Danuser G, Waterman-Storer CM. 2007 Differential transmission of actin motion within focal adhesions. *Science* **315**, 111–115. (doi:10.1126/science.1135085)
20. Lin CH, Forscher P. 1995 Growth cone advance is inversely proportional to retrograde F-actin flow. *Neuron* **14**, 763–771. (doi:10.1016/0896-6273(95)90220-1)
21. Chan CE, Odde DJ. 2008 Traction dynamics of filopodia on compliant substrates. *Science* **322**, 1687–1691. (doi:10.1126/science.1163595)
22. Choquet D, Felsenfeld DP, Sheetz MP. 1997 Extracellular matrix rigidity causes strengthening of integrin–cytoskeleton linkages. *Cell* **88**, 39–48. (doi:10.1016/S0092-8674(00)81856-5)
23. Bangasser BL, Rosenfeld SS, Odde DJ. 2013 Determinants of maximal force transmission in a motor-clutch model of cell traction in a compliant microenvironment. *Biophys. J.* **105**, 581–592. (doi:10.1016/j.bpj.2013.06.027)
24. Critchley DR. 2004 Cytoskeletal proteins talin and vinculin in integrin-mediated adhesion. *Biochem. Soc. Trans.* **32**, 831–836. (doi:10.1042/BST0320831)
25. Giannone G, Jiang G, Sutton DH, Critchley DR, Sheetz MP. 2003 Talin1 is critical for force-dependent reinforcement of initial integrin-cytoskeleton bonds but not tyrosine kinase activation. *J. Cell Biol.* **163**, 409–419. (doi:10.1083/jcb.200302001)
26. Jiang G, Giannone G, Critchley DR, Fukumoto E, Sheetz MP. 2003 Two-piconewton slip bond between fibronectin and the cytoskeleton depends on talin. *Nature* **424**, 334–337. (doi:10.1038/nature01805)
27. Zhang X, Jiang G, Cai Y, Monkley SJ, Critchley DR, Sheetz MP. 2008 Talin depletion reveals independence of initial cell spreading from integrin activation and traction. *Nat. Cell Biol.* **10**, 1062–1068. (doi:10.1038/ncb1765)
28. Ezzell RM, Goldmann WH, Wang N, Parasharama N, Ingber DE. 1997 Vinculin promotes cell spreading by mechanically coupling integrins to the cytoskeleton. *Exp. Cell Res.* **231**, 14–26. (doi:10.1006/excr.1996.3451)
29. Alenghat FJ, Fabry B, Tsai KY, Goldmann WH, Ingber DE. 2000 Analysis of cell mechanics in single vinculin-deficient cells using a magnetic tweezer. *Biochem. Biophys. Res. Commun.* **277**, 93–99. (doi:10.1006/bbrc.2000.3636)
30. Thievessen I *et al*. 2013 Vinculin-actin interaction couples actin retrograde flow to focal adhesions, but is dispensable for focal adhesion growth. *J. Cell Biol.* **202**, 163–177. (doi:10.1083/jcb.201303129)
31. Hirata H, Tatsumi H, Lim CT, Sokabe M. 2014 Force-dependent vinculin binding to talin in live cells: a crucial step in anchoring the actin cytoskeleton to focal adhesions. *Am. J. Physiol. Cell Physiol.* **306**, C607–C620. (doi:10.1152/ajpcell.00122.2013)
32. Lee SE, Kamm RD, Mofrad MRK. 2007 Force-induced activation of talin and its possible role in focal adhesion mechanotransduction. *J. Biomech.* **40**, 2096–2106. (doi:10.1016/j.jbiomech.2007.04.006)
33. Hytönen VP, Vogel V. 2008 How force might activate talin's vinculin binding sites: SMD reveals a structural mechanism. *PLoS Comput. Biol.* **4**, e24. (doi:10.1371/journal.pcbi.0040024)
34. del Rio A, Perez-Jimenez R, Liy R, Roca-Cusachs P, Fernandez JM, Sheetz MP. 2009 Stretching single talin rod molecules activates vinculin binding. *Science* **323**, 638–641. (doi:10.1126/science.1162912)
35. Papagrigoriou E *et al*. 2004 Activation of a vinculin-binding site in the talin rod involves rearrangement of a five-helix bundle. *EMBO J.* **23**, 2942–2951. (doi:10.1038/sj.emboj.7600285)
36. Fillingham I, Gingras AR, Papagrigoriou E, Patel B, Emsley J, Critchley DR, Roberts GCK, Barsukov IL. 2005 A vinculin binding domain from the talin rod unfolds to form a complex with the vinculin head. *Structure* **13**, 65–74. (doi:10.1016/j.str.2004.11.006)
37. Vicente-Manzanares M, Zareno J, Whitmore L, Choi CK, Horwitz AF. 2007 Regulation of protrusion, adhesion dynamics, and polarity by myosins IIA and IIB in migrating cells. *J. Cell Biol.* **176**, 573–580. (doi:10.1083/jcb.200612043)
38. Choi CK, Vicente-Manzanares M, Zareno J, Whitmore LA, Mogilner A, Horwitz AR. 2008 Actin and α-actinin orchestrate the assembly and maturation of nascent adhesions in a myosin II motor-independent manner. *Nat. Cell Biol.* **10**, 1039–1050. (doi:10.1038/ncb1763)
39. Beningo KA, Dembo M, Kaverina I, Small JV, Wang YL. 2001 Nascent focal adhesions are responsible for the generation of strong propulsive forces in migrating fibroblasts. *J. Cell Biol.* **153**, 881–887. (doi:10.1083/jcb.153.4.881)
40. Landau LD, Lifshitz EM. 1986 *Theory of elasticity*, 3rd edn. Oxford, UK: Pergamon Press.
41. Gardel ML, Schneider IC, Aratyn-Schaus Y, Waterman CM. 2010 Mechanical integration of actin and adhesion dynamics in cell migration. *Annu. Rev. Cell Dev. Biol.* **26**, 315–333. (doi:10.1146/annurev.cellbio.011209.122036)
42. Margadant F, Chew LL, Hu X, Yu H, Bate N, Zhang X, Sheetz MP. 2011 Mechanotransduction *in vivo* by repeated talin stretch-relaxation events depends upon vinculin. *PLoS Biol.* **9**, e1001223. (doi:10.1371/journal.pbio.1001223)
43. Schwingel M, Bastmeyer M. 2013 Force mapping during the formation and maturation of cell adhesion sites with multiple optical tweezers. *PLoS ONE* **8**, e54850. (doi:10.1371/journal.pone.0054850)
44. Gingras AR *et al*. 2008 The structure of the C-terminal actin-binding domain of talin. *EMBO J.* **27**, 458–469. (doi:10.1038/sj.emboj.7601965)
45. Gardel ML, Sabass B, Ji L, Danuser G, Schwarz US, Waterman CM. 2008 Traction stress in focal adhesions correlates biphasically with actin retrograde flow speed. *J. Cell Biol.* **183**, 999–1005. (doi:10.1083/jcb.200810060)
46. Kilian KA, Bugarija B, Lahn BT, Mrksich M. 2010 Geometric cues for directing the differentiation of mescenchymal stem cells. *Proc. Natl Acad. Sci. USA* **107**, 4872–4877. (doi:10.1073/pnas.0903269107)
47. Jain N, Iyer V, Kumar A, Shivashankar GV. 2013 Cell geometric constraints induce modular gene-expression patterns via redistribution of HDAC3 regulated by actomyosin contractility. *Proc. Natl Acad. Sci. USA* **110**, 11 349–11 354. (doi:10.1073/pnas.1300801110)
48. Prager-Khoutorsky M, Lichtenstein A, Krishnan R, Rajendran K, Mayo A, Kam Z, Geiger B, Bershadsky AD. 2011 Fibroblast polarization is a matrix-rigidity-dependent process controlled by focal adhesion mechanosensing. *Nat. Cell Biol.* **13**, 1457–1465. (doi:10.1038/ncb2370)
49. Nicolas A, Geiger B, Safran SA. 2004 Cell mechanosensitivity controls the anisotropy of focal adhesions. *Proc. Natl Acad. Sci. USA* **101**, 12 520–12 525. (doi:10.1073/pnas.0403539101)
50. Bruinsma R. 2005 Theory of force regulation by nascent adhesion sites. *Biophys. J.* **89**, 87–94. (doi:10.1529/biophysj.104.048280)
51. Shemesh T, Bershadsky AD, Kozlov MM. 2012 Physical model for self-organization of actin cytoskeleton and adhesion complexes at the cell front. *Biophys. J.* **102**, 1746–1756. (doi:10.1016/j.bpj.2012.03.006)